Electronic, vibrational, and superconducting properties of CaBeSi: First-principles calculations

C. Bersier,[1,2] A. Floris,[1,2] A. Sanna,[1,2,3] G. Profeta,[4] A. Continenza,[4] E. K. U. Gross,[1,2] and S. Massidda[3]
[1]*Institut für Theoretische Physik, Freie Universität Berlin, Arnimallee 14, D-14195 Berlin, Germany*
[2]*European Theoretical Spectroscopy Facility (ETSF)*
[3]*Department of Physics, University of Cagliari and Sardinian Laboratory for Computational Materials Science SLACS (INFM-CNR), Cittadella Universitaria, I-09024 Monserrato (Ca), Italy*
[4]*Dipartimento di Fisica, CNISM, Università degli Studi dell'Aquila, Via Vetoio 10, I-67010 Coppito (L'Aquila), Italy*
(Received 7 November 2008; published 4 March 2009)

We report first-principles calculations on the normal and superconducting state of $CaBe_xSi_{2-x}$ ($x=1$), in the framework of density-functional theory for superconductors. CaBeSi is isostructural and isoelectronic to MgB_2 and this makes possible a direct comparison of the electronic and vibrational properties and the electron-phonon interaction of the two materials. Despite many similarities with MgB_2 (e.g., σ and π bands at the Fermi level and an even larger density of states), according to our calculations CaBeSi has a very low critical temperature $T_c \approx 0.4$ K consistent with the experiment. CaBeSi exhibits a complex gap structure, with three gaps at the Fermi level: besides the σ and π gaps (present also in MgB_2), the appearance of a third gap is related to the anisotropy of the Coulomb repulsion, acting in different ways on the bonding and antibonding electronic π states.

DOI: 10.1103/PhysRevB.79.104503 PACS number(s): 74.25.Jb, 63.22.Np, 74.70.Ad, 71.15.Mb

I. INTRODUCTION

The complexity and the fragility of the effective pairing interaction—the result of a fine interplay of opposite contributions—and its nontrivial dependence on chemical properties make the search for new superconducting materials a very difficult task, even within the class of phonon-mediated superconductors. As a result, research often goes along the lines of searching in the "neighborhood" of known superconductors. This has been the case of MgB_2 that owes its superconducting (SC) properties[1–3] essentially to the presence of holes in the sp^2 σ B-B covalent bonds, strongly coupled with the E_{2g} stretching mode. During the last years, MgB_2 boosted experimental and theoretical research in the class of diborides, layered, and graphitelike materials; all sharing some hopefully relevant features with the "parent compound." Although this effort did not succeed in finding superconductors with better (or at least equivalent) properties than MgB_2, it led to the experimental discovery of some new superconductors such as graphite-intercalated compounds,[4,5] boron-doped diamond,[6] and to some theoretical proposals.[7,8]

Among MgB_2-like materials, one interesting case is represented by $CaSi_2$, which at ambient pressure has a rhombohedral structure and changes to a trigonal phase between ≈ 7 and 9.5 GPa. At $P > 16$ GPa, $CaSi_2$ has the AlB_2 structure and SC critical temperatures (T_c) up to 14 K. The stability of the AlB_2 phase at ambient pressure is achieved through hole doping. The stabilization process has been related[9] to the filling of the π antibonding bands (π_a). Let us consider a material CaX_xSi_{2-x} (X having a lower valence than Si): increasing x from zero introduces holes in the π_a bands, with a change in the X-Si bond that from an sp^3-like character acquires a progressive sp^2 character, stabilizing the AlB_2 structure.[9] Thus, hole-doped $CaSi_2$ could represent (with some differences) a good candidate for a MgB_2-like material, although its stabilization at high pressure poses some problems. Nevertheless, experimentally, the AlB_2 phase was observed at ambient pressure by doping $CaSi_2$ with Al (Refs. 10 and 11) or—in a much less studied case—with Be.[12,13] Recently, $CaBe_xSi_{2-x}$ was investigated in the doping range $0.5 \leq x \leq 1$ (Ref. 13) and was observed to have the AlB_2 structure at $x=0.75$ (Refs. 12 and 13) and, against the expectations, not to be a superconductor down to 4.2 K.[13]

The goal of this paper is to clarify why this happens despite the presence of σ holes—as in MgB_2—and an even larger density of states at the Fermi energy. We investigate the normal and SC phase of $CaBe_xSi_{2-x}$ at $x=1$ (CaBeSi in the following),[14] in the AlB_2 phase, with Be and Si atoms alternating within the honeycomb layers with an *AA* stacking.

The paper is organized as follows. In Secs. II and III we sketch our computational framework and describe the details of our calculations. In Sec. IV we illustrate the normal-state properties and the electron-phonon (e-ph) coupling of CaBeSi. The superconducting properties are discussed in Sec. V. Finally, in Sec. VI, we summarize our results.

II. DENSITY-FUNCTIONAL THEORY FOR SUPERCONDUCTORS

The superconducting properties are studied within the density-functional theory for superconductivity (SCDFT) (Refs. 15 and 16): a completely parameter free approach which allows one to predict the SC gap and T_c values of real materials.[15,16] As the SCDFT method was discussed in full detail in previous papers,[15,16] here we only sketch the main points concerning the theory, whose central result is the generalized self-consistent gap equation,

$$\Delta_{n\mathbf{k}} = -\mathcal{Z}_{n\mathbf{k}}\ \Delta_{n\mathbf{k}} - \frac{1}{2}\sum_{n'\mathbf{k}'} \mathcal{K}_{n\mathbf{k},n'\mathbf{k}'} \frac{\tanh((\beta/2)E_{n'\mathbf{k}'})}{E_{n'\mathbf{k}'}} \Delta_{n'\mathbf{k}'}, \quad (1)$$

where n and $\mathbf{k}$ are, respectively, the electronic band index and the Bloch wave vector; $\Delta_{n\mathbf{k}}$ is the SC gap function; β is the inverse temperature; $E_{n\mathbf{k}} = \sqrt{(\varepsilon_{n\mathbf{k}} - \mu)^2 + |\Delta_{n\mathbf{k}}|^2}$ are the SC quasiparticle energies defined in terms of the gap function, the Kohn-Sham eigenenergies $\varepsilon_{n\mathbf{k}}$ of the normal state, and

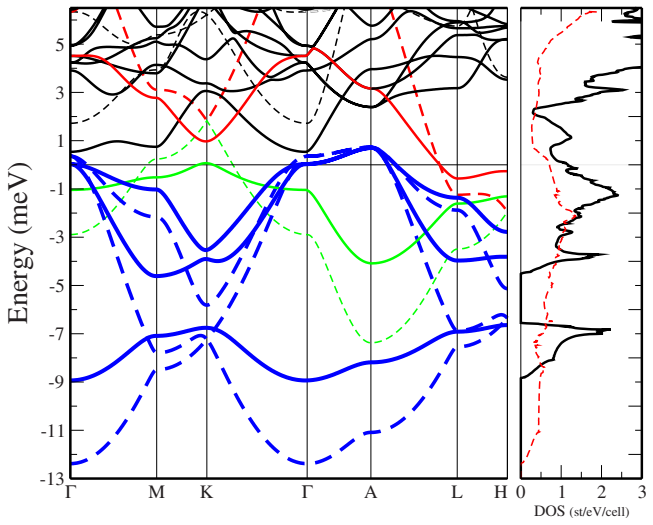

FIG. 1. (Color online) Band structure and DOS of CaBeSi (full lines) and MgB_2 (dashed lines). Different line-styles (colors) refer to different characters: σ (blue/thick lines), π bonding (green/light gray), and π antibonding (red/dark gray).

the chemical potential μ. The *universal* kernel $\mathcal{K}_{\boldsymbol{nk},n'\boldsymbol{k}'}$ appearing in Eq. (1) consists of two contributions $\mathcal{K}=\mathcal{K}^{\text{e-ph}}+\mathcal{K}^{\text{e-e}}$, representing the effects of the e-ph and the electron-electron (e-e) interactions, respectively. $\mathcal{K}^{\text{e-ph}}$ is temperature dependent and involves the e-ph coupling matrix elements $|g^{nn'}_{\boldsymbol{k},\boldsymbol{k}',\nu}|^2$ and the phonon spectrum $\omega_{\boldsymbol{q}\nu}$, while $\mathcal{K}^{\text{e-e}}$ contains the matrix elements of the screened Coulomb repulsion. Finally, the *universal* diagonal (and temperature dependent) term $\mathcal{Z}_{\boldsymbol{nk}}$ plays a similar role as the renormalization term in the Eliashberg equations. We emphasize that Eq. (1) is not a mean-field equation (as in BCS theory), since it contains correlation effects via the SC exchange-correlation (xc) functional entering $\mathcal{K}$ and $\mathcal{Z}$. Furthermore, it has the form of a static equation—i.e., it does not depend *explicitly* on the frequency—and therefore has a simpler structure (and is computationally more manageable) than the Eliashberg equations. However, this certainly does not imply that retardation effects are absent from the theory. Once again, retardation effects enter through the xc functional, as explained in Refs. 15 and 16.

An important feature of the SCDFT approach is the capability to include the $\boldsymbol{nk}$-resolved Coulomb repulsion $V^{\text{e-e}}$ *ab initio* without any adjustable parameter. The Coulomb interaction was screened with a static dielectric matrix, within the random phase approximation (RPA) (Ref. 17) (see below).

III. COMPUTATIONAL DETAILS

The electronic band structure $\varepsilon_{\boldsymbol{nk}}$, the phonon spectrum $\omega_{\boldsymbol{q}\nu}$, and the e-ph and Coulomb matrix elements (MEs) with respect to the Bloch functions necessary to determine the SC gap from Eq. (1) were obtained within the plane-wave-pseudopotential method.[18] We used Troullier-Martins[19] norm-conserving pseudopotentials[20] with $2s$, $3s$-$3p$, and $3s$-$3p$-$4s$ for Be, Si, and Ca, respectively, in the generalized gradient approximation (GGA) as parametrized in Ref. 21 for the xc functional. The electronic self-consistent cycle was performed with a 60 Ry energy cutoff and a 18^3 Monkhorst-Pack $\boldsymbol{k}$-point mesh.

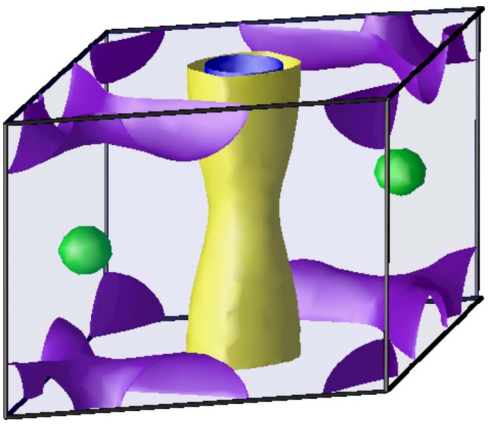

FIG. 2. (Color online) CaBeSi Fermi surface. The colors identify the three gaps at E_F: the largest σ (yellow and blue cylindrical-like sheets); the intermediate π bonding (green spheres); and the lowest π antibonding (violet).

The optimized lattice parameters (at $x=1$ Be doping) are $a=3.895$ Å and $c/a=1.112$, whereas the experimental values (at $x=0.75$) are $a=3.94$ Å and $c/a=1.112$.[12,13] Our obtained slightly smaller GGA-PBE a constant is justified by the larger amount of Be (with smaller covalent radius than Si) present in the calculated system.

Phonons and e-ph MEs were calculated via density-functional perturbation theory.[22] The phonons were computed on the irreducible set of a regular mesh of 8^3 $\boldsymbol{q}$ points and 16^3 Monkhorst-Pack $\boldsymbol{k}$ points for electronic integration, with a smearing parameter of 0.35 eV. These parameters were sufficient to achieve convergence within 0.5 meV in the frequency of the $E_{2g}(\Gamma)$ mode. Our calculated $\omega_{E_{2g}}(\Gamma)=59.0$ meV compares well with the value $\omega_{E_{2g}}(\Gamma)=57.1$ meV obtained by frozen phonon calculations in Ref. 9 computed at the slightly larger $a=3.914$ Å. The e-ph ME were calculated on the same $\boldsymbol{q}$-point grid as the phonons and on a denser grid of 24^3 $\boldsymbol{k}$ points, while the RPA-screened Coulomb MEs were calculated[17] on a mesh of $9^3\times 9^3$ $\boldsymbol{k}$ and $\boldsymbol{k}'$ points. The SC gap function is extremely peaked around the Fermi surface (FS) (within the characteristic phonon energy), whereas at higher energies it is rather smooth (and it changes sign, due to the e-e interaction). This implies that a converged solution of Eq. (1) needs a denser $\boldsymbol{k}$-point sampling around E_F, while a coarser one is sufficient elsewhere. This highly nonuniform mesh of the Brillouin zone (BZ) is realized with 8×10^3 and 500 independent $\boldsymbol{k}$ points for bands crossing and not crossing the Fermi level, respectively. Finally, 15–20 self-consistent iterations were sufficient to achieve a complete convergence of the gap.

IV. NORMAL-STATE PROPERTIES

A. Electronic structure and Fermi surface

Figure 1 shows the CaBeSi and MgB_2 band structures. A general similarity is found: in both materials the σ,

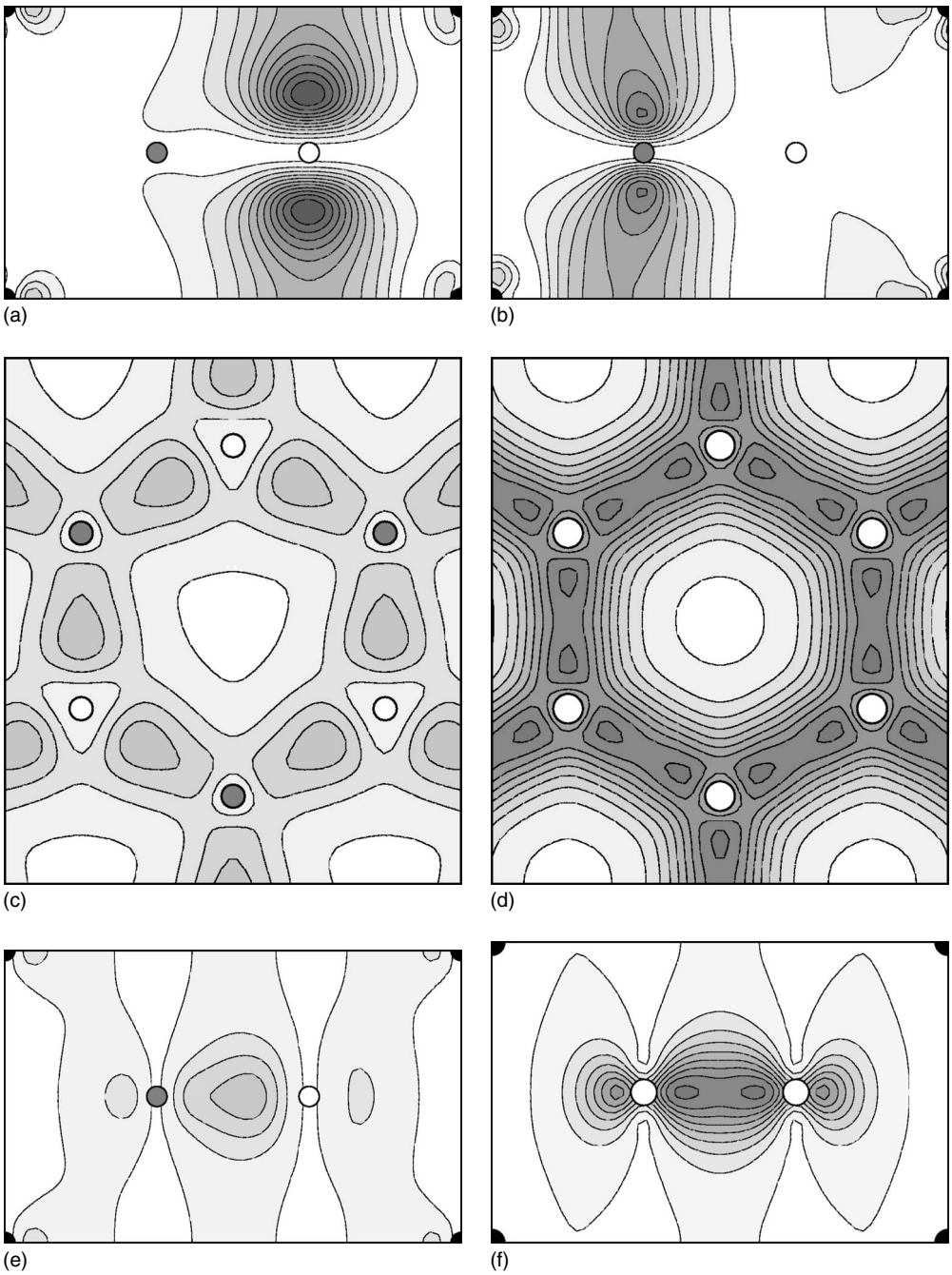

FIG. 3. CaBeSi and MgB_2 charges. Upper panel: CaBeSi π bonding (left) and π antibonding (right) charges at the H point; empty (full) circle refers to Si (Be). Middle and lower panels: CaBeSi (left) and MgB_2 (right) σ charges at the Γ point; in the middle (lower) panel, the z direction is perpendicular (parallel) to the page.

π-bonding (π_b), and π-antibonding (π_a) bands cross the Fermi level (E_F). As pointed out in Ref. 9 and similarly to CaAlSi,[23] the reduced symmetry (space group $P\bar{6}m2$) with respect to MgB_2 ($P6/mmm$) related to the partially ionic nature of the B-Si bond implies the splittings of the σ and the π_b-π_a bands at the K and H points of the BZ. In CaBeSi the π_b bands are almost fully occupied, leaving only small hole pockets at K which give rise to the little π spheres of the FS (see Fig. 2). These replace the π tubular structure present in MgB_2. The π_a bands are only partially occupied, allowing the stabilization of the Si-Be sp^2 network against an sp^3-like distortion. In fact, the latter takes place in the presence of a larger amount of Si, i.e., with a larger filling of the π_a bands.[9]

Due to the different electronegativity of Si and Be, we expect a change in the charge distribution related to their bond, in comparison with the B-B bond in MgB_2. In Fig. 3 (upper panel), we plot the π_b and π_a charges at the BZ H point. We see that the π_b (π_a) charge is clearly associated to the Si (Be) atom. Having in mind the different occupation of the π_b and π_a bands, we conclude that there is a charge disproportion in favor of Si.

TABLE I. Structural parameters (in Å) of CaBeSi and MgB_2.

	a	c	Si-Si	Si-Be	B-B
CaBeSi	3.895	4.331	3.895	2.249	
MgB_2 [a]	3.083	3.52			1.780

[a]Experimental constants.

Another important chemical difference between MgB_2 and CaBeSi is the presence of Ca d states at ~5 eV above E_F that strongly interact with π and σ bands, in different ways along the zone. This contributes to the reduced in-plane π bandwidth (≈1.1 eV and ≈2.8 eV along ΓMK and ALH) in CaBeSi with respect to MgB_2 (≈5.5 eV). In fact, while at the Γ point there is no interaction between π states and the cation d orbitals, the interaction is possible in the high-symmetry points A, M, and K, therefore suppressing the large dispersion of these states observed in MgB_2. However, the main reason for the larger MgB_2 band dispersion (see Fig. 1) is its smaller unit cell with respect to CaBeSi (volume effect) which affects both π and σ states.

Looking at the σ charge in the two materials (Fig. 3, middle and lower panels), we notice a stronger localization in MgB_2 along the B-B direction; whereas in CaBeSi the σ charge has a clear ionic component and is more delocalized both in the in-plane and out-of-plane directions. This makes the Si-Be bond much weaker than the B-B one affecting the strength of the e-ph coupling.

As far as the σ bandwidth is concerned, the larger Si-Be distance (see Table I) and a lower Si-Be interaction (compared to B-B) explain the reduced in-plane σ-band dispersion (for the lower σ≈5 eV and ≈8 eV in CaBeSi and MgB_2, respectively). On the other hand, the larger out-of-plane dispersion of σ bands in CaBeSi (≈1 eV) versus MgB_2 (≈0.5 eV) is only partially justified with the larger z extension of the CaBeSi σ charge (compensated by the ≈25% larger interlayer distance), and is mainly related to the $\sigma-\mathrm{Ca}\ d_{x^2-y^2}$ interaction allowed at the Γ point but not at A (see Fig. 1). The difference in band dispersion gives rise to much of the warping of the corresponding Fermi surface.

B. Phonons and electron-phonon coupling

The previous discussion shows that despite the general similarities, CaBeSi and MgB_2 have rather different chemical and electronic properties. As expected, they determine both the vibrational properties and the electron-phonon coupling. In fact, CaBeSi frequencies are lower (see Fig. 4) in comparison with MgB_2, mainly due to the larger mass of Ca and Si versus Mg and B.

The E_{2g} mode is fairly flat along the in-plane BZ symmetry lines and it shows only a very weak renormalization along $M\Gamma$ and AH lines [four times smaller than in MgB_2 (Refs. 3, 24, and 25)] due to the very small E_{2g} electron-phonon matrix elements. In turn, this is related to the delocalized and ionic nature of the σ bonds in CaBeSi (see Fig. 3). In fact, the connection between strongly covalent bonds and strong e-ph coupling seems to be a general feature.[1,26–28]

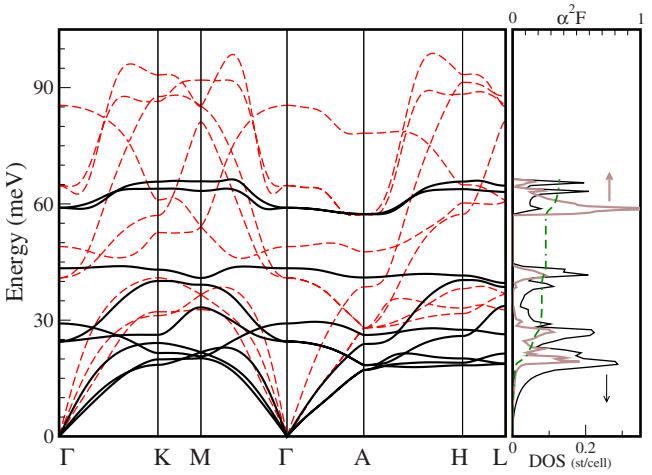

FIG. 4. (Color online) Left panel: phonon structure of CaBeSi (full lines) and MgB_2 (dashed lines). Right panel: CaBeSi phonon DOS (thin black line), Eliashberg function (thick brown line), and integration curve $2\int_0^\omega \alpha^2F(\omega')/\omega' d\omega'$ (dot-dashed green line), whose final value is the total e-ph coupling λ.

The B_{1g} mode is lower than the E_{2g} everywhere in the BZ, without exhibiting the features found in CaAlSi, where it is very soft, due to a strong interband coupling between the interlayer and π_a states.[23]

The strongly reduced e-ph renormalization of the CaBeSi E_{2g} mode is not related to poor FS nesting features in this material but only to the small value of the e-ph MEs themselves. In fact, we have calculated the σ nesting function $\eta_{\mathbf{q}}^{\sigma}=\frac{1}{N_\sigma(0)}\Sigma_{\mathbf{k}\in\sigma}\delta(\epsilon_{\mathbf{k}})\delta(\epsilon_{\mathbf{k}+\mathbf{q}})$ [where $\mathbf{k}+\mathbf{q}\in\sigma$ and $N_\sigma(0)$ is the σ density of states (DOS) at E_F], obtaining *larger* values for CaBeSi than for MgB_2 (by roughly a factor of 2).

The calculated total e-ph is λ=0.38, which makes CaBeSi a weak-coupling superconductor, comparable to Al or Mo, with a T_c=0.4 K. The two-band-resolved values [see Eq. (3)] are $\lambda_{\sigma\sigma}$=0.29, $\lambda_{\sigma\pi}$=0.21, $\lambda_{\pi\sigma}$=0.15, and $\lambda_{\pi\pi}$=0.12 whereas the MgB_2 values are[29] $\lambda_{\sigma\sigma}$=0.83, $\lambda_{\sigma\pi}$=0.22, $\lambda_{\pi\sigma}$=0.16, and $\lambda_{\pi\pi}$=0.28.

Further insights on this dramatic reduction of $\lambda_{\sigma\sigma}$ in CaBeSi are obtained by looking at the σ deformation potential δ related to the E_{2g} mode at the Γ point.[30] For CaBeSi we obtained δ≈6 eV/Å, while the value 13 eV/Å is found in MgB_2. This difference derives partly from the different lattice parameters, influencing the σ bandwidths, and partly from the different nature of the bond in the two compounds. In fact, a test calculation for CaBeSi using the MgB_2 lattice parameters gives the intermediate value δ=9.5 eV/Å.

Although weaker than in MgB_2, the contribution from the E_{2g} mode is important also in the CaBeSi Eliashberg function (Fig. 4), where we see a peak at ~60 meV, which strongly enhances a corresponding structure in the phonon density of states. This peak gives roughly one fourth of the total e-ph coupling, while the main contribution comes from low-frequency modes.

We note that charge localization not only enhances the e-ph interaction but also the Coulomb MEs,[31] which are lower in CaBeSi than in MgB_2. However, this reduction is not so dramatic as for the e-ph MEs. This is due to the

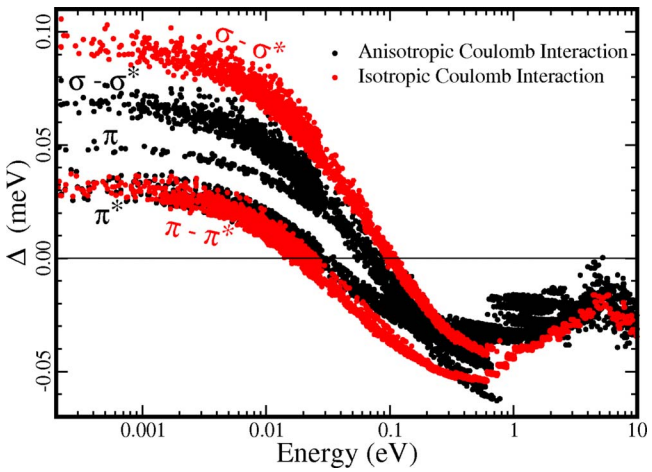

FIG. 5. (Color online) CaBeSi superconducting gap as a function of the energy distance from the Fermi level.

different structure of the MEs of the two interactions (see discussion below).

V. SUPERCONDUCTING STATE

The solution of the self-consistent gap equation [Eq. (1)] including the anisotropic e-ph MEs $|g^{nn'}_{\mathbf{k},\mathbf{k}',\nu}|^2$ and the $n\mathbf{k}$-resolved RPA Coulomb matrix elements $V^{\text{e-e}}_{n\mathbf{k},n'\mathbf{k}'}$ reveals an unexpected complex structure with clearly separated *three* gaps at E_F (Fig. 5). The calculated critical temperature is very low (T_c=0.4 K), lower than the upper limit (4.2 K) set by the experimental results.[13] Unlike in MgB_2, in which superconductivity is interpreted within a two-band model,[2,32–34] in CaBeSi there is a further π_b-π_a gap splitting. As in MgB_2, the largest gap is related to the σ FS sheets (cylindrical-like structures in Fig. 2), the intermediate one to π_b sheets (small hole spheres), and the lowest to π_a sheets. The additional π_b-π_a gap splitting is a peculiar feature of CaBeSi not present in MgB_2, where the two σ and the two π gaps merge together. In order to understand the origin of this splitting, we performed some additional computational experiments, solving the gap equation (i) completely neglecting the Coulomb interaction, (ii) including only the averaged Coulomb term,

$$V^{\text{e-e}}_{av}(\epsilon,\epsilon') = \frac{1}{N(\epsilon)N(\epsilon')} \sum_{n\mathbf{k},n'\mathbf{k}'} V^{\text{e-e}}_{n\mathbf{k},n'\mathbf{k}'} \times \delta(\epsilon_{n\mathbf{k}} - \epsilon)\delta(\epsilon_{n'\mathbf{k}'} - \epsilon'), \quad (2)$$

and (iii) with isotropically averaged Coulomb and phononic interactions, corresponding to the dirty limit.

In both (i) and (ii) cases, the three-gap structure is destroyed, bringing back a two-band MgB_2-like gap structure. In case (iii), instead, superconductivity is completely lost. As a result, we predict superconductivity in CaBeSi *only* if the anisotropic structure of the interactions is included. In the real system, very likely, disorder on the Si-Be sublattice can produce interband π-σ impurity scattering, therefore reducing T_c further.

TABLE II. (a) Band-resolved density of states [st/(cell eV)]. (b) Band-resolved e-ph couplings $\lambda_{nn'}$ (in bold) and BCS effective potentials $V^{\text{e-ph}}_{nn'}=\lambda_{nn'}/N'_n$ [in parentheses (eV)]. (c) Band-resolved e-e interactions at the Fermi energy $\mu_{nn'}$ (in bold), and e-e matrix elements $V^{\text{e-e}}_{nn'}$ at the Fermi energy [in parentheses (eV)].

(a)

DOS	σ_1	σ_2	π_b	π_a
N	0.12	0.38	0.1	0.58

(b)

e-ph	σ_1	σ_2	π_b	π_a
σ_1	**0.07** (0.62)	**0.23** (0.61)	**0.03** (0.28)	**0.20** (0.34)
σ_2	**0.07** (0.61)	**0.22** (0.57)	**0.02** (0.23)	**0.19** (0.32)
π_b	**0.03** (0.28)	**0.09** (0.23)	**0.03** (0.35)	**0.16** (0.28)
π_a	**0.04** (0.34)	**0.12** (0.32)	**0.03** (0.28)	**0.07** (0.12)

(c)

e-e	σ_1	σ_2	π_b	π_a
σ_1	**0.11** (0.91)	**0.27** (0.71)	**0.03** (0.30)	**0.15** (0.26)
σ_2	**0.08** (0.71)	**0.32** (0.84)	**0.03** (0.29)	**0.13** (0.23)
π_b	**0.04** (0.30)	**0.11** (0.29)	**0.09** (0.94)	**0.20** (0.35)
π_a	**0.03** (0.26)	**0.09** (0.23)	**0.03** (0.35)	**0.51** (0.86)

In the following we will analyze the three-gap structure, with particular emphasis in understanding the π_b-π_a splitting. To this purpose, we perform a four-band model analysis, splitting the Fermi surface in the internal σ band (σ_1), external σ band (σ_2), and π_b and π_a bands.

We calculated (see Table II) the corresponding density of states N_n and the BCS-like e-ph couplings $\lambda_{nn'}$ and $V^{\text{e-ph}}_{nn'}$, where

$$\lambda_{nn'} = V^{\text{e-ph}}_{nn'} N_{n'} \quad (3)$$

and

$$V^{\text{e-ph}}_{nn'} = \frac{2}{N_n N_{n'}} \sum_{\mathbf{k}\in n,\mathbf{k}'\in n'} \sum_{\nu} \frac{|g^{nn'}_{\mathbf{k},\mathbf{k}',\nu}|^2}{\omega_{\mathbf{k}'-\mathbf{k},\nu}} \delta(\varepsilon_{n\mathbf{k}})\delta(\varepsilon_{n'\mathbf{k}'}). \quad (4)$$

First, we notice that the σ submatrix $V^{\text{e-ph}}_{\sigma\sigma}$ is very homogeneous. Second, the σ-π scattering gives the same contribution to both σ gaps, which are then identical. Superconductivity in the π states is more complicated, essentially because—unlike the σ bands—π_a and π_b bands originate from different sublattices. As a consequence, the π subma-

trix is not homogeneous. Moreover, the π-σ interaction is of the same size as the π-π one and π_a and π_b have different density of states, being $N_{\pi_a} \simeq 6N_{\pi_b}$. In order to understand the qualitative structure of the SCDFT results, we considered a BCS-type approximation of the four-band Eliashberg equations.[35] This model calculation confirms that the inclusion of the average Coulomb interaction [Eq. (2)] does not produce π_b-π_a gap splitting. In fact, the splitting is recovered *only* considering the (band) anisotropic $V^{\text{e-e}}_{nn'}$ Coulomb MEs reported in Table II. These are—as for the el-ph coupling—roughly homogeneous in the σ submatrix and therefore not able to split the σ gap; but in the $V^{\text{e-e}}_{\pi\pi}$ submatrix, the intraband interaction is $\approx$2.7 times larger than the interband interaction (that couples states in different sublattices). The huge difference between $V^{\text{e-e}}_{\pi_b\pi_a}$ and $V^{\text{e-e}}_{\pi_a\pi_a}$ and the low N_{π_b} (that makes the $\mu_{\pi_b\pi_b}$ and $\mu_{\pi_a\pi_b}$ negligible) leads to a much stronger suppression of Δ_{π_a} relative to Δ_{π_b}, ultimately leading to the three-gap structure.

VI. SUMMARY AND CONCLUSIONS

We have calculated the normal and superconducting state properties of $CaBe_xSi_{2-x}$ ($x=1$) in the AlB_2 phase, within the SCDFT. The chosen doping level is not far from the experimental doping ($x=0.75$) where this phase is found stable and homogeneous. CaBeSi is isostructural and isoelectronic to MgB_2 and the electronic, vibrational properties and electron-phonon interaction of the two materials are compared directly. While the band structures present strong similarities, with both σ and π bands crossing the Fermi level, the phonon structure and the e-ph interaction differ substantially. In particular, the less-localized σ charge of CaBeSi leads to a dramatic reduction in the E_{2g} electron-phonon coupling, with a consequent reduction in the phonon renormalization seen in MgB_2. This fact makes CaBeSi a weak-coupling superconductor with e-ph $\lambda=0.38$ and $T_c=0.4$ K, in spite of a density of states at the Fermi surface twice as big as in MgB_2. Our analysis shows that the presence of superconductivity in CaBeSi is entirely due to anisotropy. For isotropically averaged Coulomb and phononic interactions (corresponding to the dirty limit), superconductivity disappears completely. Interestingly, CaBeSi exhibits three superconducting gaps at the Fermi level. While, as in MgB_2, the σ-π gap splitting is related to the different e-ph coupling in these bands, the further π_b-π_a splitting is a pure effect of the complex anisotropic structure of the Coulomb repulsion, acting in different ways on the π_b and π_a states.

ACKNOWLEDGMENTS

The authors thank A. Marini for technical support and for making the SELF code available. This work was supported by the Italian Ministry of Education through a 2004 PRIN project by the Istituto Nazionale di Fisica della Materia (INFM-CNR) through a supercomputing grant at Cineca (Bologna, Italy), by MIUR under project PONCyberSar, by the Deutsche Forschungsgemeinschaft, by the EXCITING Network, and by the NANOQUANTA Network of Excellence. A.F. acknowledges CNISM for financial support during his visit to the University of L'Aquila. A.S. acknowledges the financial support from the Master and Back program of the *Regione Autonoma della Sardegna*. C.B. acknowledges financial support from the Swiss National Science Foundation.

[1] J. M. An and W. E. Pickett, Phys. Rev. Lett. **86**, 4366 (2001).
[2] A. Y. Liu, I. I. Mazin, and J. Kortus, Phys. Rev. Lett. **87**, 087005 (2001).
[3] Y. Kong, O. V. Dolgov, O. Jepsen and O. K. Andersen, Phys. Rev. B **64**, 020501(R) (2001).
[4] T. E. Weller, M. Ellerby, S. S. Saxena, R. P. Smith, and N. T. Skipper, Nat. Phys. **1**, 39 (2005).
[5] N. Emery, C. Hérold, M. d'Astuto, V. Garcia, Ch. Bellin, J. F. Marêché, P. Lagrange, and G. Loupias, Phys. Rev. Lett. **95**, 087003 (2005).
[6] E. A. Ekimov, V. A. Sidorov, E. D. Bauer, N. N. Mel'nik, N. J. Curro, J. D. Thompson, and S. M. Stishov, Nature (London) **428**, 542 (2004).
[7] H. Rosner, A. Kitaigorodsky, and W. E. Pickett, Phys. Rev. Lett. **88**, 127001 (2002).
[8] F. J. Ribeiro and M. L. Cohen, Phys. Rev. B **69**, 212507 (2004).
[9] G. Satta, G. Profeta, F. Bernardini, A. Continenza, and S. Massidda, Phys. Rev. B **64**, 104507 (2001).
[10] M. Imai, K. Nishida, T. Kimura, and H. Abe, Appl. Phys. Lett. **80**, 1019 (2002).
[11] B. Lorenz, J. Lenzi, J. Cmaidalka, R. L. Meng, Y. Y. Sun, Y. Y. Xue, and C. W. Chu, Physica C **383**, 191 (2002).
[12] N. May, W. Müller, and H. Schäfer, Z. Naturforsch. B **2**, 1947 (1977).
[13] F. Sano, Y. Takahashi, K. Takase, Y. Takano, and K. Sekizawa, CP850 Low Temperature Physics: 24th International Conference on Low Temperature Physics, AIP Conf. Proc. **850**, 641 (2006).
[14] The chosen doping $x=1$ is not far from the experimental stoichiometry ($x=0.75$) and avoids cumbersome supercell approaches and problems related to Be and Si orderings.
[15] M. Lüders, M. A. L. Marques, N. N. Lathiotakis, A. Floris, G. Profeta, L. Fast, A. Continenza, S. Massidda, and E. K. U. Gross, Phys. Rev. B **72**, 024545 (2005).
[16] M. A. L. Marques, M. Lüders, N. N. Lathiotakis, G. Profeta, A. Floris, L. Fast, A. Continenza, E. K. U. Gross, and S. Massidda, Phys. Rev. B **72**, 024546 (2005).
[17] SELF code, http://www.fisica.uniroma2.it/~self/
[18] All calculations have been performed with the QUANTUM-ESPRESSO package (http://www.quantum-espresso.org/). Reliability of the used pseudopotentials has been checked against all electron calculations using the EXCITING code (http://exciting.sourceforge.net/).
[19] N. Troullier and J. L. Martins, Phys. Rev. B **43**, 1993 (1991).
[20] M. Fuchs and M. Scheffler, Comput. Phys. Commun. **119**, 67

(1999); http://www.fhi-berlin.mpg.de/th/fhi98md/fhi98PP/

[21] J. P. Perdew, K. Burke, and M. Ernzerhof, Phys. Rev. Lett. **77**, 3865 (1996).

[22] S. Baroni, S. de Gironcoli, A. Dal Corso, and P. Giannozzi, Rev. Mod. Phys. **73**, 515 (2001).

[23] M. Giantomassi, L. Boeri, and G. B. Bachelet, Phys. Rev. B **72**, 224512 (2005).

[24] K. P. Bohnen, R. Heid, and B. Renker, Phys. Rev. Lett. **86**, 5771 (2001).

[25] A. Shukla, M. Calandra, M. d'Astuto, M. Lazzeri, F. Mauri, C. Bellin, M. Krisch, J. Karpinski, S. M. Kazakov, J. Jun, D. Daghero, and K. Parlinski, Phys. Rev. Lett. **90**, 095506 (2003).

[26] G. Profeta, C. Franchini, N. N. Lathiotakis, A. Floris, A. Sanna, M. A. L. Marques, M. Lüders, S. Massidda, E. K. U. Gross, and A. Continenza, Phys. Rev. Lett. **96**, 047003 (2006).

[27] A. Sanna, C. Franchini, A. Floris, G. Profeta, N. N. Lathiotakis, M. Lüders, M. A. L. Marques, E. K. U. Gross, A. Continenza, and S. Massidda, Phys. Rev. B **73**, 144512 (2006).

[28] A. Floris, A. Sanna, S. Massidda, and E. K. U. Gross, Phys. Rev. B **75**, 054508 (2007).

[29] A. Floris, A. Sanna, G. Profeta, N. N. Lathiotakis, M. Lüders, M. A. L. Marques, C. Franchini, E. K. U. Gross, A. Continenza, and S. Massidda, Physica C **456**, 45 (2007).

[30] We used the definition $\delta=\frac{1}{2}\frac{\Delta\epsilon_{\mathrm{gap}}}{\Delta u_B}$, where u_B is the B displacement along the E_{2g} mode and $\Delta\epsilon_{\mathrm{gap}}$ is the induced σ band splitting.

[31] In MgB_2, for example, the strong hole-doped covalent B-B bond ensures a high el-ph coupling: however, an equally high repulsive Coulomb interaction reduces the superconducting critical temperature.

[32] A. Brinkman, A. A. Golubov, H. Rogalla, O. V. Dolgov, J. Kortus, Y. Kong, O. Jepsen, and O. K. Andersen, Phys. Rev. B **65**, 180517(R) (2002).

[33] A. A. Golubov, A. Brinkman, O. V. Dolgov, J. Kortus, and O. Jepsen, Phys. Rev. B **66**, 054524 (2002).

[34] O. V. Dolgov, R. S. Gonnelli, G. A. Ummarino, A. A. Golubov, S. V. Shulga, and J. Kortus, Phys. Rev. B **68**, 132503 (2003).

[35] E. Macocian, Mod. Phys. Lett. B **19**, 503 (2005).